Available online at www.sciencedirect.com
ScienceDirect
Journal of Sound and Vibration 322 (2009) 135–154
JOURNAL OF SOUND AND VIBRATION
www.elsevier.com/locate/jsvi

Fuzzy modal analysis: Prediction of experimental behaviours

F. Massa*, T. Tison, B. Lallemand

Laboratoire d'Automatique de Mécanique et d'Informatique industrielles et Humaines, Université de Valenciennes, Le Mont Houy B.P. 311, 59313 Valenciennes, France

Received 6 February 2008; received in revised form 22 October 2008; accepted 28 October 2008
Handling Editor: C.L. Morfey
Available online 21 December 2008

Abstract

The objective of this paper is to numerically predict the modal behaviours of a two-plate steel structure defined with variable parameters and to validate this prediction experimentally. First, the test structure, in which geometrical and material variability has been identified, is studied using a Fuzzy Finite Element Method. This method, named PAEM, allows the fuzzy numerical eigenfrequencies and eigenvectors to be calculated. Second, the test structure is analyzed experimentally to quantify the possible variation of the eigensolutions' modal behaviours and to build the experimental fuzzy sets. Finally, the fuzzy numerical quantities are compared with the experimental quantities to highlight the efficiency of our non-deterministic model for predicting the behavioural modifications of the test structure.

1. Introduction

Recent progress in computing resources has allowed increasingly complex and realistic numerical models to be exploited. For example, it is now possible to simulate mechanical structures with very large numbers of finite elements, to realise multiphysics applications and to take imperfections into account. Previously, when creating and using new structures, the sources of deficiencies that had been identified for different parameters were never taken into account in the numerical simulations, and all design parameters were considered deterministically. These deficiencies can be defined by the term ''imperfection'' and two classes can be distinguished. Variability refers to the variation inherent to the physical system or the environment under consideration. Uncertainty is a potential deficiency in any phase or activity of the modelling process that is due to lack of knowledge.

Different theories, both probabilistic and non-probabilistic, have thus been developed to manage the imperfections mentioned above. Among the non-probabilistic theories [1], the fuzzy set theory allows both imprecise data and subjective data to be modelled. This fuzzy formalism has been coupled with the finite element method (FFEM [2–5]) and has already been employed successfully to solve a variety of increasingly complex problems (e.g., static [6], modal [7–9], dynamic [10–16], design and optimisation [6,17,18], identification [19], multi-body [20]). These studies have led to many numerical applications that have not

*Corresponding author. Tel.: +33 327511459; fax: +33 327511317.
E-mail address: franck.massa@univ-valenciennes.fr (F. Massa).

0022-460X/$ - see front matter
doi:10.1016/j.jsv.2008.10.032

always been compared to a numerical reference (e.g., Zadeh's Extension Principle) and never to an experimental reference.

This paper compares fuzzy numerical and experimental data, with the goal of numerically predicting the variation of modal behaviour. This prediction is made using a nominal model and an estimation of the different variability parameters, and then the prediction is validated experimentally. To successfully complete the study described in this paper, many data were needed to efficiently determine the fuzzy numerical and experimental database:

- A modular test structure in which some element of variability can be identified.
- An efficient Fuzzy Finite Element Method to propagate the variability.
- Specific experimental modal analyses to build the fuzzy experimental reference.

Section 2 introduces the two-plate steel structure used in our experiments, its corresponding finite element model, and our experimental process. In Section 3, the main sources of imperfections in non-deterministic analysis are described. Section 4 presents the fuzzy formalism and its coupling with the Finite Element Method, and reviews the PAEM method, presented previously in Ref. [2]. In Section 5, the fuzzy numerical and experimental results are compared in terms of fuzzy eigenvalues and eigenvectors in order to demonstrate the capacity of the fuzzy model to represent imperfections. The final section offers our conclusions and perspectives for future research.

2. Description of the two-plate steel structure

The example considered in this paper is the two-plate steel structure presented in Fig. 1. Both plates in the structure were honed and screwed together with eight Chc M4 bolts and then glued to avoid assembly defects. The material properties, geometric characteristics and the associated measurement tolerances are specified in Section 3, which describes and quantifies the various imperfections. The finite element model of the nominal structure (Fig. 2) contains 400 shell elements and 2706 degrees of freedom. This configuration was chosen in order to allow the first five elastic mode shapes to be studied. The neutral planes of the plates were defined as the middle of the thickness measurement.

Experimental modal analyses were performed to determine the structure's first five elastic mode shapes. During experimentation, the structure was suspended using four standard springs. Fig. 3 shows the position of the excitation points and the accelerometers, which were placed in accordance with the mesh nodes. Using an 8-channel acquisition system, the accelerometers were divided into two sets, corresponding to two configurations with an optimised mass distribution. Configuration 1 (dashed arrows) has 7 sensors and

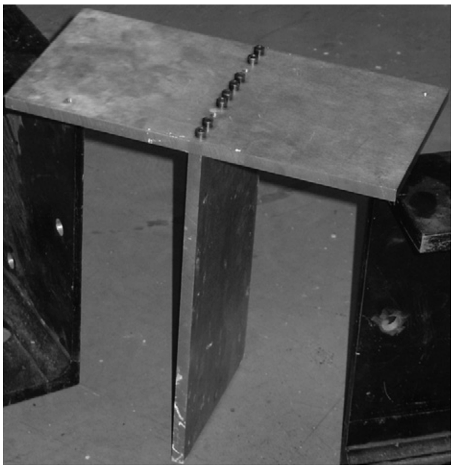

Fig. 1. Two-plate steel structure.

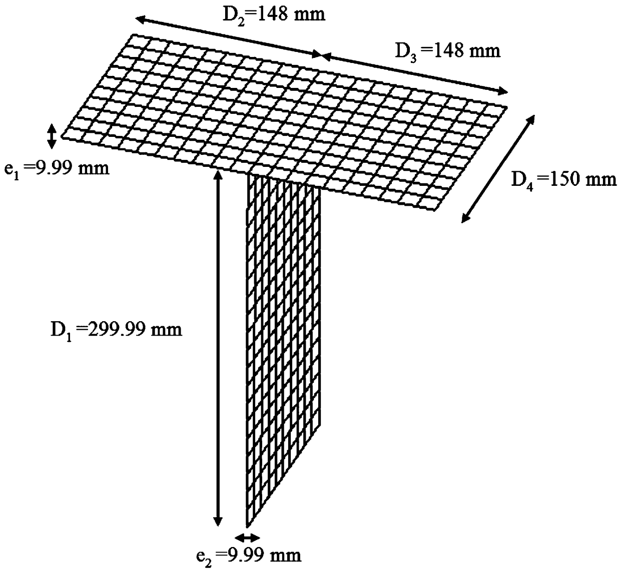

Fig. 2. Finite-element model of the test structure.

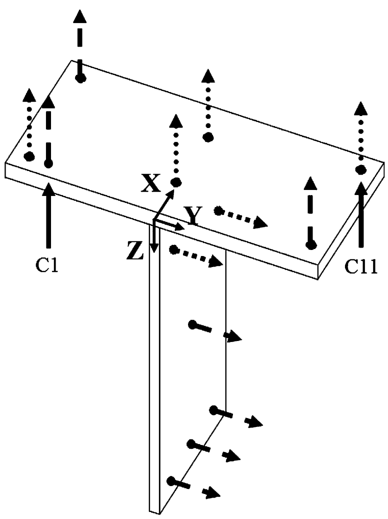

Fig. 3. Sensor model of the test structure. ⟶ Excitation ‒ ‒► Accelerometers (Configuration 1) ···► Accelerometers (Configuration 2).

configuration 2 (dotted arrows) has 6 sensors. For this experimentation, only 13 measurement directions, selected by the effective independence method [21], are sufficient to clearly distinguish the reduced mode shapes using the Modal Assurance Criterion (MAC). The MAC is obtained using the following equation:

$$\mathrm{MAC}_{(\phi_1,\phi_2)} = \frac{\|\phi_1^{\mathrm{T}}\phi_2\|^2}{(\phi_1^{\mathrm{T}}\phi_1)(\phi_2^{\mathrm{T}}\phi_2)} \quad (1)$$

where ϕ_1 and ϕ_2 are two mode shapes to be compared. Generally, MAC values ranging from 0.8 or 0.9 to 1 are considered to define a good correlation between two mode shapes, especially for numerical data. Below this limit, notable differences can appear locally in the mode shape, leading to a permutation between frequencies. As Fig. 4 shows, for both configurations, all criteria are near 1 and the mode shapes are correctly separated.

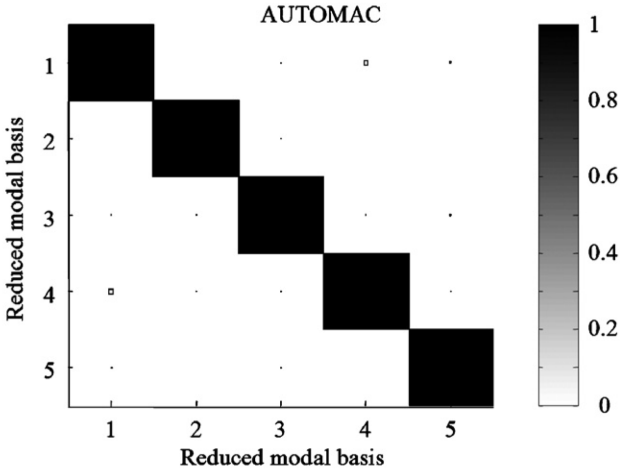

Fig. 4. AUTOMAC for reduced modal bases.

For this experimentation, only one excitation point is necessary to excite correctly all the modes of the structure in the studied frequency range. Nevertheless, to increase the confidence about results and to quantify the measurement quality, all the tests are successively realized for two different excitation points (C1 and C11). More details about the validity and repeatability of these tests are provided in Section 3.

Throughout the study described in this paper, the plate thickness is assumed to be variable, with an imprecision of $\pm 20\%$ in the nominal thickness values. To insure a variable plate thickness, three vertical and three horizontal plates were manufactured, and the plate measurements were used to construct a database. The thickness imperfections were voluntarily exaggerated in order to obtain large variations in the eigenfrequencies and to prevent small variations in the eigenfrequencies from being interpreted as possible measurement errors.

3. Imperfections in non-deterministic analysis

There are three main types of imperfections: experimental, modelling and parametric. Experimental imperfections generally originate in the test conditions and the calibration of the different sensors used. Modelling imperfections stem from the process of discretizing the structure using finite element theory and the different simplifications employed when building the model. Parametric imperfections come from the material and geometric parameters or loads and represent the different observed dispersions.

In this study, only the last type of imperfection is considered. The influence of the first two types of imperfections was reduced by defining a rigorous protocol, as described in the following paragraphs.

3.1. Experimental imperfections

To obtain accurate Frequency Response Functions (FRF) and decrease the possible imperfections, different precautions were taken into account during the experimental process. A stepped sine below 1000 Hz with a variable frequency step was used to concentrate the information around the resonance frequencies. For example, the Fig. 5 highlights the quality of the results for an accelerometer placed beside the excitation point C1. Appropriation criteria [22] were then employed to detect the resonance and to calculate the best frequency step. These criteria allow the FRFs to be fitted more reliably, thus making the identification phase easier (Fig. 6). To verify the variation in the measurements, the impedance measurements were compared for the two sensor configurations. Fig. 7 shows the very good stability of the measurements for the different series, and Fig. 8 highlights the good linearity of the overall behaviour according to Maxwell's reciprocity principle. Still, there is a small gap in the fifth eigenfrequency. Table 1 summarizes the frequency measurements obtained at the two excitation points and the errors for the two configurations. As this table shows, the maximal frequency

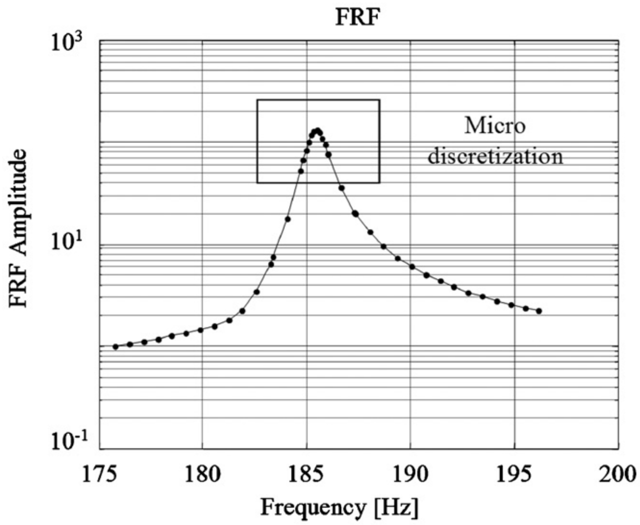

Fig. 5. Micro discretization around the first mode (results presented to excitation point C1).

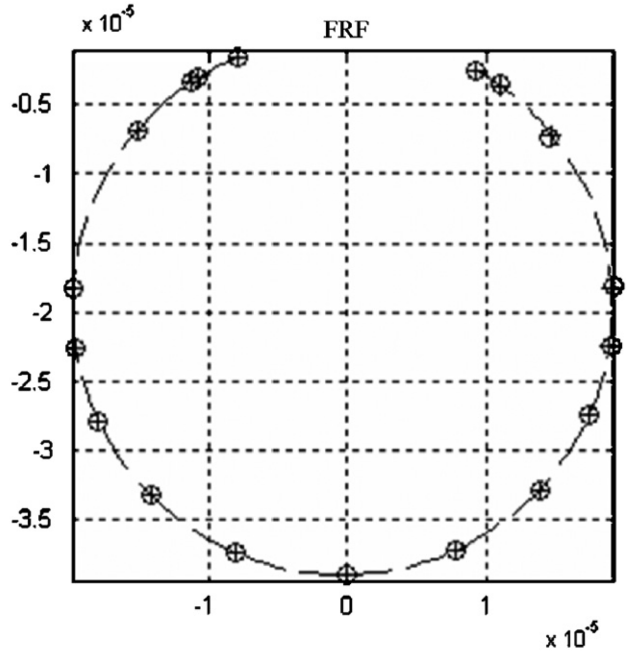

Fig. 6. Comparison of the measured "o" and calculated "+" Nyquists for the first mode.

error is less than 1%. Repeating the tests revealed a rise in the observed mean frequency deviation to 0.3%, which implies good measurement repeatability. To further quantify the closeness of two correlated mode shapes, two scaled vector errors are defined as follows:

$$\mathrm{err}_{\mathrm{N}(\%)} = \frac{\|\phi_1\| - \|\phi_2\|}{\|\phi_1\|}, \quad \text{norm error, for a global overview} \tag{2}$$

$$\mathrm{err}_{\mathrm{RN}(\%)} = \frac{\|\phi_1 - \phi_2\|}{\|\phi_1\|}, \text{ norm error difference, mainly for highlighting local errors} \tag{3}$$

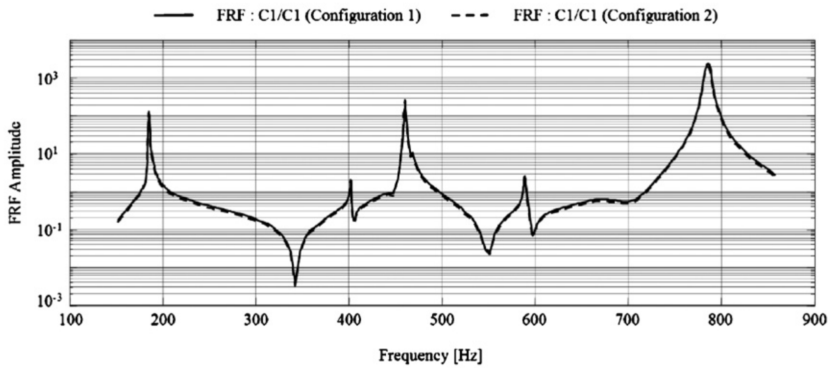

Fig. 7. Impedance measurements for the two sensor configurations (point C1). —— FRF: C1/C1 (Configuration 1) – – – FRF: C1/C1 (Configuration 2).

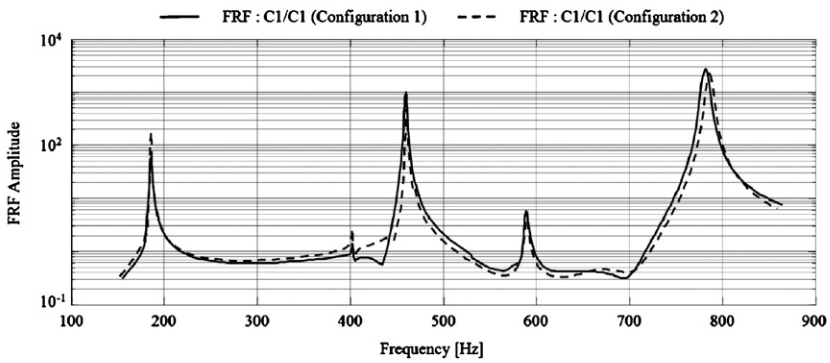

Fig. 8. Maxwell's reciprocity principle as applied to the FRFs C1/C11 and C11/C1. —— FRF: C1/C1 (Configuration 1) – – – FRF: C1/C1 (Configuration 2).

Table 1
Experimental frequencies and errors between points C1 and C11 in the nominal test structure.

	f_1	f_2	f_3	f_4	f_5
Excitation C1 (Hz)	185.42	402.84	459.80	587.81	786.62
Excitation C11 (Hz)	185.17	402.30	458.48	586.38	780.24
Errors (%)	0.1	0.1	0.3	0.2	0.8
	ϕ_1	ϕ_2	ϕ_3	ϕ_4	ϕ_5
Errors N (%)	1.2	3.2	11.5	0.8	8.1
Errors RN (%)	2.0	4.5	13.1	6.9	20.1

where $\|\cdot\|$ is the Euclidian norm and ϕ_1 and ϕ_2 are two mode shapes to be compared (for example experimental and numerical mode shapes).

The pairing of the mode shapes for the two configurations is also very good. As shown in Fig. 9, the MAC criteria are superior to 0.97 for each mode shape (Fig. 9), and the mean error between the eigenvectors is on the order of 9% (Table 1). Although the experimental protocol is rigorous, the identification of the fifth mode is very difficult. The Fig. 8 shows a small variation of the fifth resonance between the two configurations (C1 and C11). This variation implies necessarily an error level observed in Table 1. Nevertheless, as the MAC criterion is superior to 0.97 and the error level, observed by the norm error difference, is equal to 20%, the

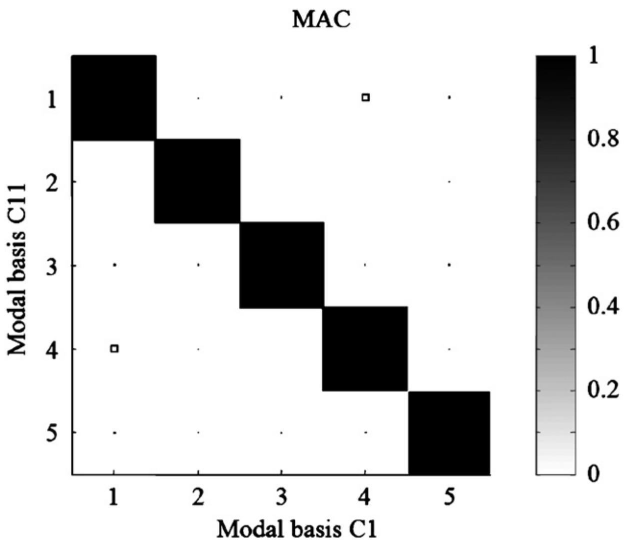

Fig. 9. MAC criteria for the modal bases obtained at C1 and C11.

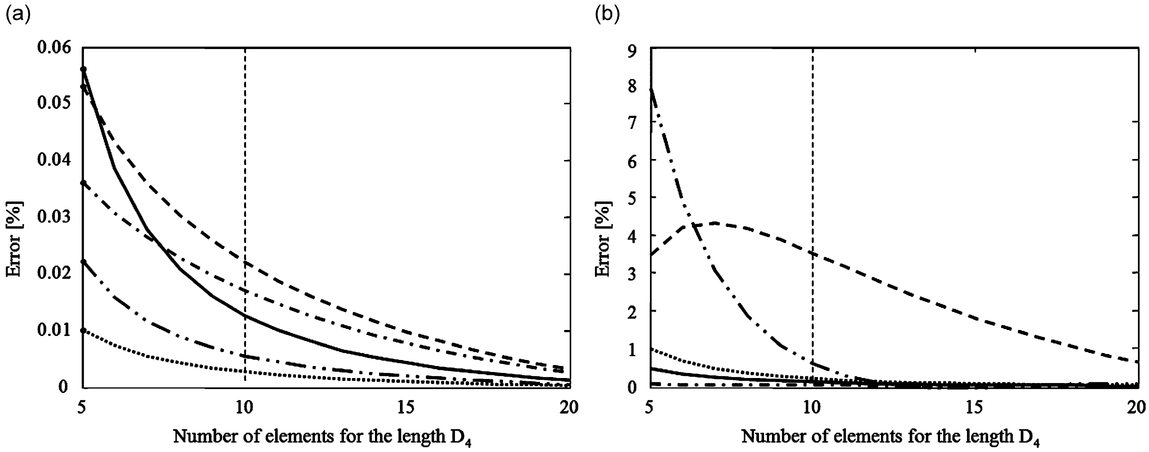

Fig. 10. Convergence of eigensolutions in relation to the number of finite-elements. (a) frequencies ········ f1 —— f2 —· · f3 — · – f4 ––– f5 and (b) degree of freedom of sensor C1 ········ mode 1 —— mode 2 —· · mode 3 — · – mode 4 ––– mode 5.

authors are considered the results as acceptable. Moreover, the numerical simulation shows that this fifth mode is difficult to precisely calculate. The convergence of the fifth eigensolution (Fig. 10) is not very good. The error level does not decrease even if the number of elements for the length D_4 increases. This fifth mode is more difficult to interpret than the others.

3.2. Modelling imperfections

To create a simple but representative finite element model, several precautions were taken. The two plates in each test structure were glued with epoxy adhesive and assembled with eight bolts in order to obtain as close a fit as possible. Torque repeatability was guaranteed by using a torque wrench for each test structure. The finite element model was based on the results of our study of eigensolution convergence in relation to the number of finite elements. The basic length of an element was determined by dividing the length D_4 into 10 parts. As the convergence of the fifth mode (Fig. 10) is, however, more difficult to interpret than the others, this mode is not

Table 2
Errors made in determining the numerical and experimental frequencies and eigenvectors.

	f_1	f_2	f_3	f_4	f_5
Numerical (Hz)	185.98	403.06	460.60	589.32	777.08
Excitation C1 (Hz)	185.42	402.84	459.80	587.81	786.62
Excitation C11 (Hz)	185.17	402.30	458.48	586.38	780.24
Errors C1 (%)	0.3	0.1	0.2	0.3	1.2
Errors C11 (%)	0.4	0.2	0.5	0.5	0.4
	ϕ_1	ϕ_2	ϕ_3	ϕ_4	ϕ_5
Errors N C1 (%)	1.1	5.8	13.3	2.8	11.9
Errors RN C1 (%)	4.1	7.2	13.9	7.7	15.6
Errors N C11 (%)	2.2	2.3	1.6	2.1	18.5
Errors RN C11 (%)	4.1	5.8	5.5	8.8	19.8

Table 3
Geometric characteristic and associated variations.

Thickness e_1 (mm)	Thickness e_2 (mm)	Length D_1 (mm)
[8.04; 9.99; 12.01]	[8.04; 9.99; 12.01]	[298.49; 299.99; 301.49]
Length D_2 (mm)	Length D_3 (mm)	Length D_4 (mm)
[147.75; 148.00; 148.25]	[147.75; 148.00; 148.25]	[149.9; 150.00; 150.1]

chosen for the determination of discretization used for the length D_4. This discretization corresponds to an error inferior to 1% for the first four eigensolutions.

Since experimental and numerical data for the nominal structure were very close, it was not necessary to update the nominal model (Table 2). Thus, before introducing the different imperfections into the finite element model, the nominal numerical solutions had to be updated based on the nominal experimental data. If this had not been done, the nominal model would have lacked essential representativity, and our study would have been pointless.

3.3. Parametric imperfections

Using a parametric model allows imperfections to be taken into account. In this study, the thicknesses of the two plates in the nominal test structure were allowed to vary by 20% of the nominal thickness values. Three thicknesses (8.04, 9.99 and 12.01 mm), measured with a micrometer, were introduced to simulate different design choices. The thickness variations introduced were intentionally greater than normal production variations in order to avoid confusing the intentional variations with any inadvertent experimental variations.

Other geometric and material imperfections taken into account in this study included production variability, measurement errors, and lack of knowledge about materials. First, the different dimensions were measured using a calliper rule or a simple steel rule. The measurement tolerances were 0.1 and 0.5 mm, respectively. All geometric parameters and their associated variations are provided in Table 3. Second, the structure was manufactured in standard steel, whose the material properties were not completely known. In theory, Young's modulus ranged from 1.9×10^{11} to $2.1 \times 10^{11}\,N/m^2$, density from 7750 to 7950 Kg/m^3, and Poisson's ratio from 0.27 to 0.33 (http://www.matweb.com, http://www.efunda.com). Experiments were realized to provide some realistic variation intervals, with Young's modulus being determined with a vibrometric method [23] and density with a weighing method. The theorical associated variations of parameters were reduced and the realistic variations are presented in Table 4.

Table 4
Material properties and associated variations.

Young's modulus E (10^{11} N/m^2)	Density ρ (Kg/m^3)	Poisson's ratio ν
[2.00; 2.02; 2.06]	[7775; 7831; 7883]	[0.27; 0.30; 0.33]

4. Fuzzy numerical analysis

4.1. Fuzzy set theory

The fuzzy set theory was introduced by Zadeh [24–27] as an extension or generalisation of classic set theory. In Zadeh's theory, a membership degree, varying between 0 and 1, is associated to the different values of the non-deterministic parameters. In this context, a fuzzy number is then defined using a membership function that can take different forms, depending on the kind of imperfection considered. Without information about imperfection, triangular membership functions are the simplest and common choice. However, with additional information, other membership functions can be chosen (p-shape, trapezoidal...) to model the perception of the user [28,29]. As experimentally, the information are available for $\alpha = 0$ (nominal value) and $\alpha = 1$ (bounds of fuzzy numbers), the triangular form was chosen for each imprecise input parameter. The membership functions of nine fuzzy parameters (Fig. 11) were built using the data presented in Tables 3 and 4.

Fuzzy set theory has its own arithmetic, which allows the classic operations (e.g., $+$, $-$, $\times$) on the fuzzy scalars to be extended. Extending this arithmetic to problems with matrices or to other more complex problems (e.g., linear systems, eigenvalues) is not trivial and implies some overestimation. The solution, as described in fuzzy set theory, is to use the Extension Principle developed by Zadeh.

In practise, this Extension Principle is organised in three steps:

- Discretization of membership functions (the continuous problem is transformed by a discrete problem, in which the parameter variation domain is represented by all the possible combinations of discrete fuzzy parameter values).
- Calculation of deterministic solutions (due to all the combinations of fuzzy parameter values).
- Evaluation of the degree of confidence of all the solutions (the membership functions of the solutions are built by considering that the degree of membership of one combination is equal to the smallest degree of membership of the independent parameters in this combination. In the case of multiple occurrences of a solution, the final membership degree is equal to the maximum membership degree of the different solutions).

This principle is very attractive in a general context because it is simple to implement. It allows the output subset characterizing all the variations of the solutions studied to be defined according to a specific set application, such as linear systems or eigenvalue problems. Nevertheless, applying this principle directly in a mechanical engineering context, where finite element models are used, is less appealing because when the size of the finite element model or the number of fuzzy parameters increases, the approach rapidly becomes too time consuming. The different alternative approaches that have been proposed are described in the next section.

4.2. Fuzzy finite element method (FFEM)

The use of Zadeh's principle in the finite element context has led to the development of the Fuzzy Finite Element Method [3]. The aim is to determine the membership function of an output quantity, based on the fuzzy description of the input parameters. Computing with fuzzy numbers requires a discretization of the membership function. In this case, the discrete fuzzy numbers are obtained from cuts according to the degree of confidence (Fig. 12). For each α-cuts level, an interval $\tilde{p}^{\alpha}$ is defined by lower and upper bounds, $\underline{p}^{\alpha}$ and $\overline{p}^{\alpha}$, respectively.

$$\tilde{p}^{\alpha} = [\underline{p}^{\alpha}; \overline{p}^{\alpha}] \tag{4}$$

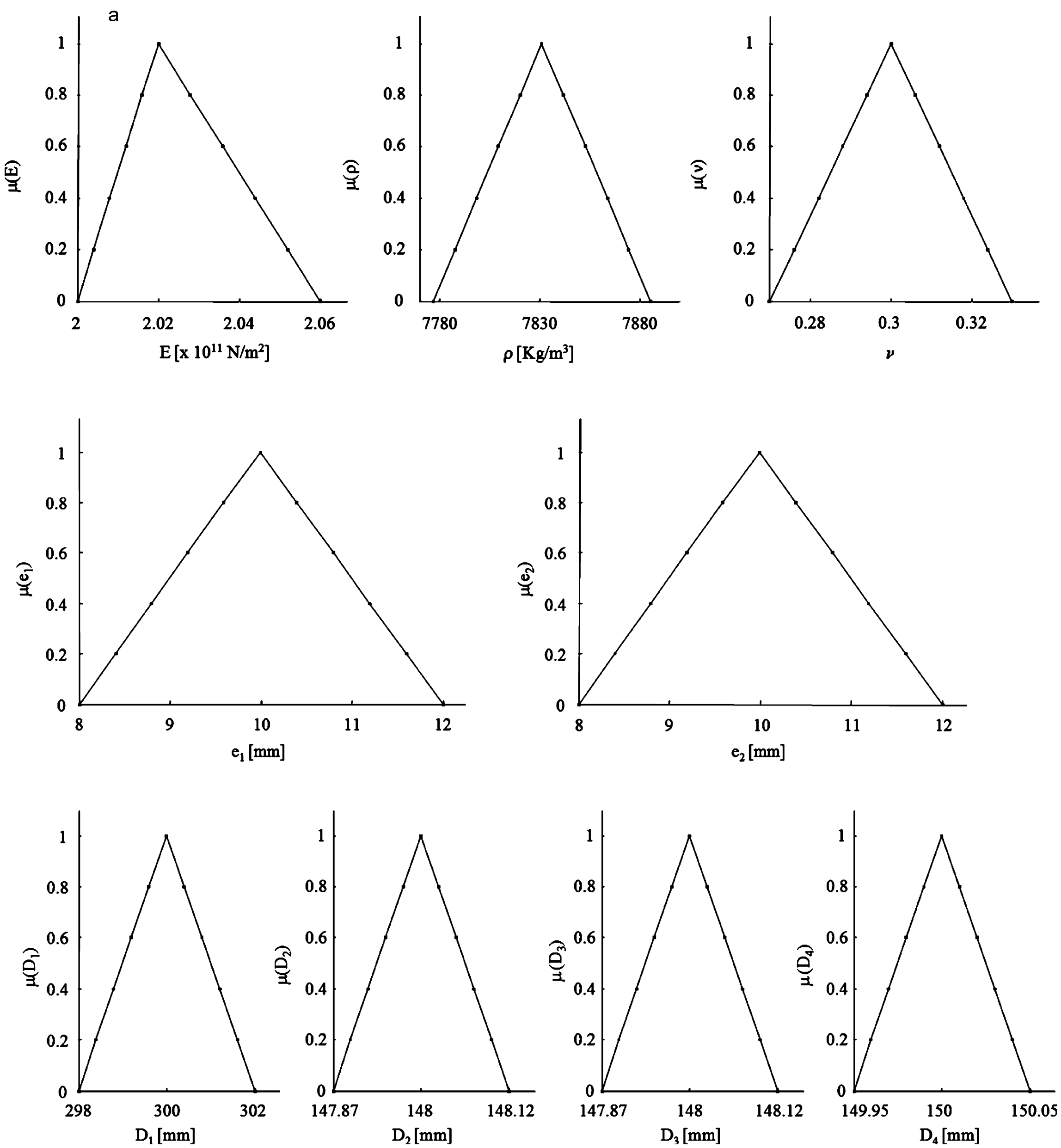

Fig. 11. Membership functions of the imprecise parameters: (a) material properties, (b) thicknesses and (c) geometric characteristics.

A maximum degree of confidence ($\alpha = 1$) was associated to the nominal value and a minimum degree of confidence ($\alpha = 0$) to the bounds of the variation interval. Using this α-sublevel technique, the membership functions of the fuzzy parameters were transformed into a set of intervals. To correctly propagate the information included in each interval, different methods have been proposed and can be divided into two main classes: global matrix formulations and parametric formulations.

In the global matrix formulation, specific interval matrices (e.g., in modal analysis, the interval mass and stiffness matrices [28]) are built for each α-cut level. The interval problem is then transformed into a first-order [9] or high-order [8] perturbed problem, and the solutions are obtained by calculating the interval bounds. These techniques, although less time consuming than the Extension

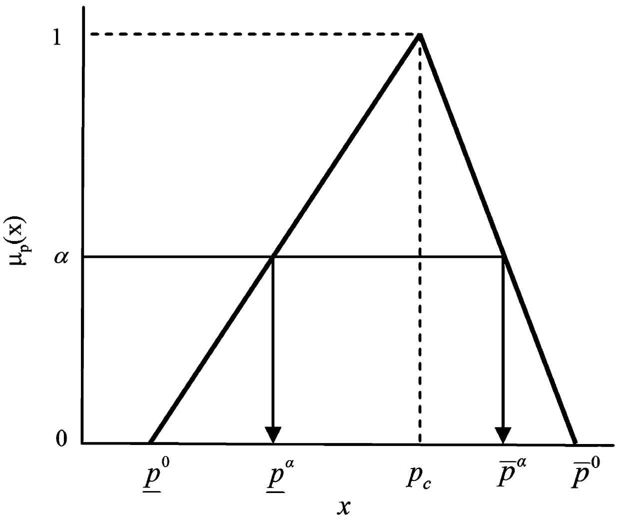

Fig. 12. Discretization of fuzzy number according to the degree of confidence.

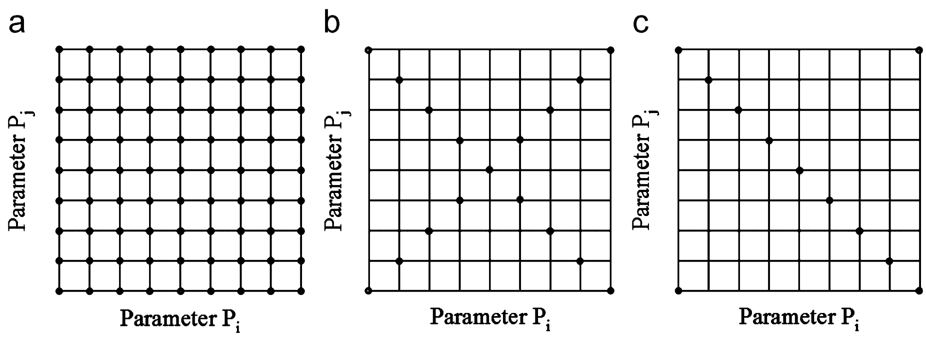

Fig. 13. Graphical representation of the different forms of the Transformation Method in the parameter space. Each black dot is an evaluated parameter combination (a) General Transformation Method (b) Reduced Transformation Method and (c) Short Transformation Method.

principle, supply only an idea of the behaviour variation but do not provide the real variations needed in the design phase.

In the parametric formulation, the interval problem is transformed into a discrete problem for each α-cut level. The overall strategy of this formulation is to look for combinations of discretized fuzzy design parameter values, which indicate the extreme variations for each α-cut level and to calculate the modified solutions for these specific parameters combinations. Amongst the proposed approaches, the Transformation Method [5] offers different forms (General, Reduced or Short) for evaluating a problem described with fuzzy formalism.

The General form is a practical implementation of Zadeh's Extension Principle as described in the fuzzy set theory. The Reduced Transformation Method [5] is an exploitation of the Vertex Method [30] for each α-cut level. A full factorial Design Of Experiment (DOE) is then performed for each of these intervals. The Short form [10] is based on the use of the Vertex Method for the support of fuzzy numbers in order to identify the principal diagonal (i.e., the diagonal in the parameter space that makes the largest contribution to the studied solutions). Graphic representations of the different Transformation Method forms in the parameter space are presented for two parameters in Fig. 13. Each black dot is an evaluated parameter combination.

In order to limit the computational cost due to managing imperfections, we have previously proposed an efficient method [2] based on sensitivity analysis, which researches the specific parameters combinations, and on a re-analysis technique, which approximates the modified solutions. The basic steps of the method, called PAEM (Padé Approximants with Extrema Management), are presented in the next section.

4.3. PAEM method

The Padé Approximants with Extrema Management (PAEM) method [2] is an extension of the Taylor Expansion with Extrema Management (TEEM) method [6]. The PAEM method was developed to respond to two specific points of eigensolution variability:

- Non-monotonic evolution: depending on the type of solutions studied (eigenvalues or eigenvectors) and the imprecise parameters involved (e.g., Young's modulus, Poisson's ratio, density, thickness), the nature of the changes in the mode shapes may be non-monotonic.
- Crossed mode shapes: the mode shapes may cross regardless of whether the nominal frequencies are distinct. Consequently, the frequencies and the mode shapes, which correspond to different parameter combinations, must be reorganised to aggregate mode shapes of the same type in the corresponding fuzzy subsets. This can be done using the MAC.

The PAEM method requires that the membership function be discretized according to the degree of confidence. The problem is then transformed into an interval problem for each α-cut level.

The PAEM algorithm follows a 2-step procedure:

- A search for parameter combinations is performed for each α-cut level, which implies minimum and maximum variations. The sensitivity of the eigensolutions is evaluated between each level to determine how the response function is evolving.
- The modified modal quantities are approximated for each selected combination. A high-order approximation using Padé rational functions is required in order to decrease the calculation time and maintain a good level of accuracy. (More information about Padé rational functions can be found in work by Elhage-Hussein et al. [31].)

Comparing the results of the PAEM method with a combinatorial reference method based on Zadeh's Extension Principle (ZEP) [24–27] underlined the efficiency of the PAEM method in terms of CPU time, bound accuracy, and the membership function forms for eigenvalues and eigenvectors. More details about the algorithm are presented in our previous article [2], and a brief review is provided in the Appendix A to this article.

5. Prediction and comparison of fuzzy eigensolutions

For the experimental tests, only the nominal values and the bounds of the interval variation for the two plate thicknesses were used. A total of nine (3×3) test structures were measured. The nine test structures were subjected to experimental modal analysis (Fig. 14). The FRFs obtained for the nine test structures are presented in Fig. 15. After identification with Modan software [32], these FRF results were then aggregated into fuzzy numbers in terms of the eigenvalues (Fig. 16) and eigenvectors, respecting the membership degree of the input parameter [19] (i.e., the results obtained for the nominal value have a degree of confidence of 1, whereas the eight other results have a degree of confidence of 0).

Before beginning the non-deterministic prediction, the most influential imprecise parameters were identified with the PAEM method in order to limit overestimating the modal solutions (Fig. 17). This preliminary step was necessary since calculating variability according to Poisson's ratio provides only a simple estimation, while characterizing Young's modulus and the density values depends on the precision of the experimental tests. This means that the variations introduced in this study are realistic, but relatively pessimistic. The thicknesses e_1 and e_2, representing 90% of the total solution, were obviously the most influential parameters in this study, which is not surprising considering the high level of variability voluntarily introduced in these parameters. Fig. 18 superimposes the first and fourth fuzzy numerical frequencies and the fuzzy experimental

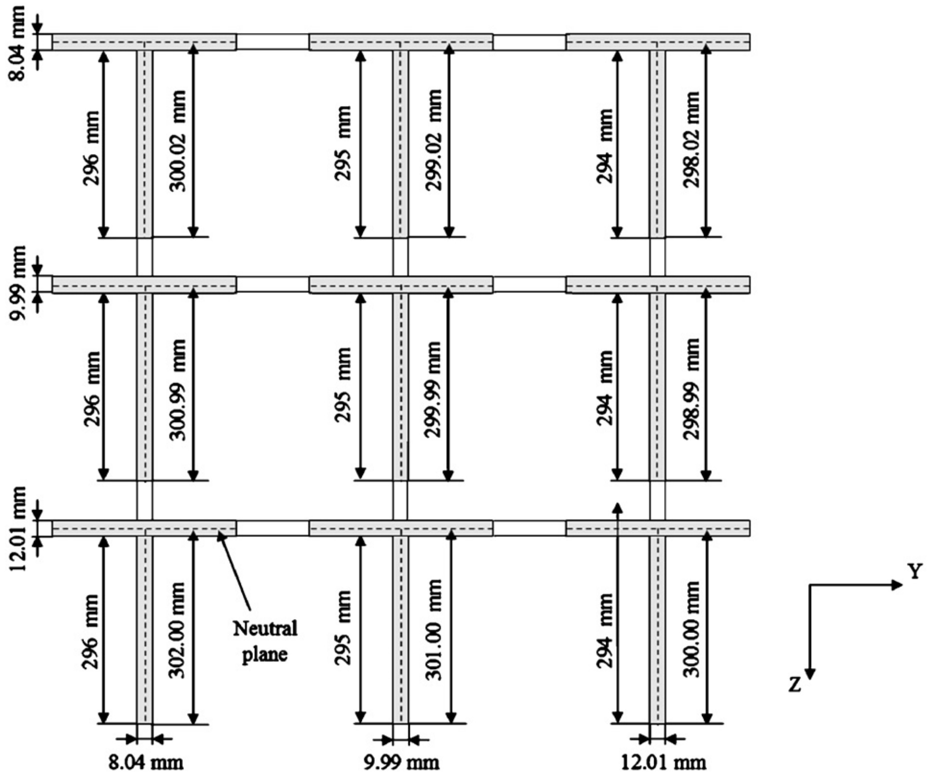

Fig. 14. Description of geometrical characteristics for the nine test structures.

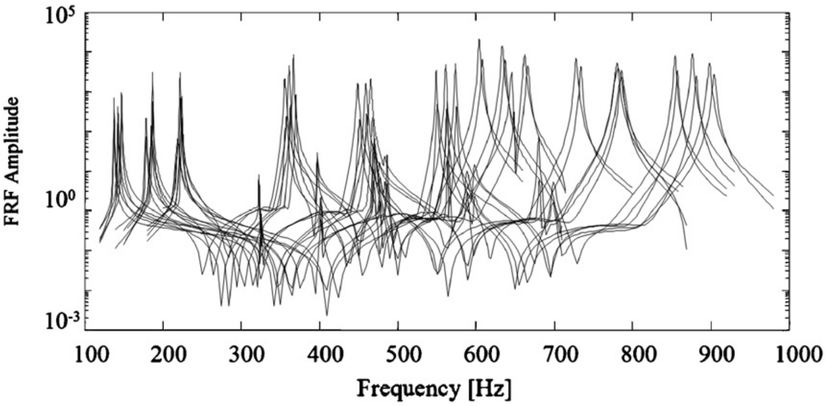

Fig. 15. FRFs obtained for the nine test structures.

frequencies (for e_1 and e_2 only). These two parameters alone are enough to show the imperfection propagated in the experimental model, but the numerical solution still slightly underestimates the lower bound of the membership functions.

Overall, the numerical results are very satisfactory. Nonetheless, if designers want to include the experimental results in the numerical results in order to take all possibilities into account, it is necessary to examine the influence of the other imprecise parameters very carefully (Fig. 19). The authors propose to use an iterative process, which adds, one by one, the most influent parameters in the PAEM methodology. The process is stopped as soon as the fuzzy numerical solution is stabilized. A careful examination of our results shows that the second-most influential parameters are the Young's modulus and the lengths D_1, D_2 and D_3.

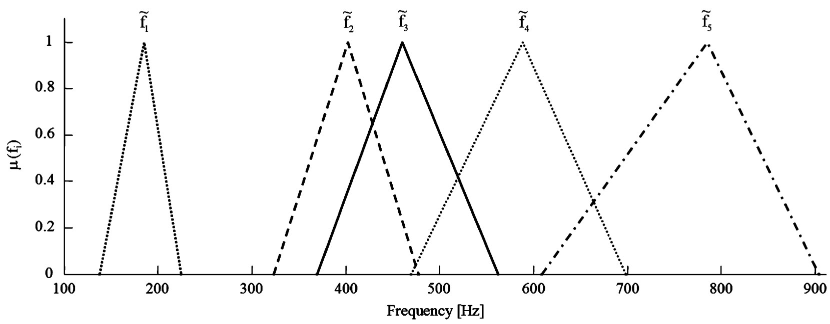

Fig. 16. Aggregation of the experimental data.

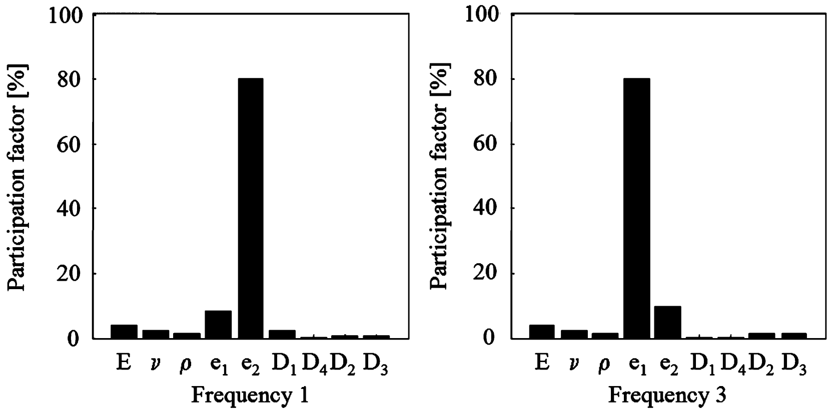

Fig. 17. Influence of imprecise parameters on frequencies f_1 and f_3.

Added to the two thickness values (e_1 and e_2), these six parameters account for 96% of the total solution. Fig. 20 superimposes the fuzzy experimental frequencies and the fuzzy numerical frequencies, determined with the six fuzzy parameters mentioned above. Fig. 21 shows the first and fourth "fuzzy" mode shapes that correspond to the upper and lower bounds of both the numerical and experimental results. The numerical results come reasonably close to the experimental data. The maximal error made in evaluating the frequency bounds is less than 5% (Fig. 22). The worst result was obtained for the fifth eigenfrequency, no doubt because both the model and the measurements for this mode shape contain errors. The results obtained for the eigenvectors are also quite interesting: the lower and upper bounds are correctly evaluated, except for the upper plate in the fourth mode shape.

The comparison of the numerical and experimental fuzzy eigenvalues and eigenvectors confirmed the usefulness of our numerical method. The results could be made even more accurate by refining the uncertainties with regard to Young's modulus, which is the most influential parameter after thicknesses.

6. Conclusion

The objective of this study was to compare numerical and experimental modal data when varied structural parameters were considered. Many experimental modal analyses were completed for nine test structures using specific values of imprecise parameters, and the results were then aggregated to fuzzy eigensolutions. Numerically, the imperfections of the fuzzy parameters were propagated using the PAEM method in order to obtain fuzzy eigensolutions. Using a good quality nominal model and a reasonable estimate of the variability of the significant parameters, we were able to demonstrate a good correspondence between numerical and experimental data.

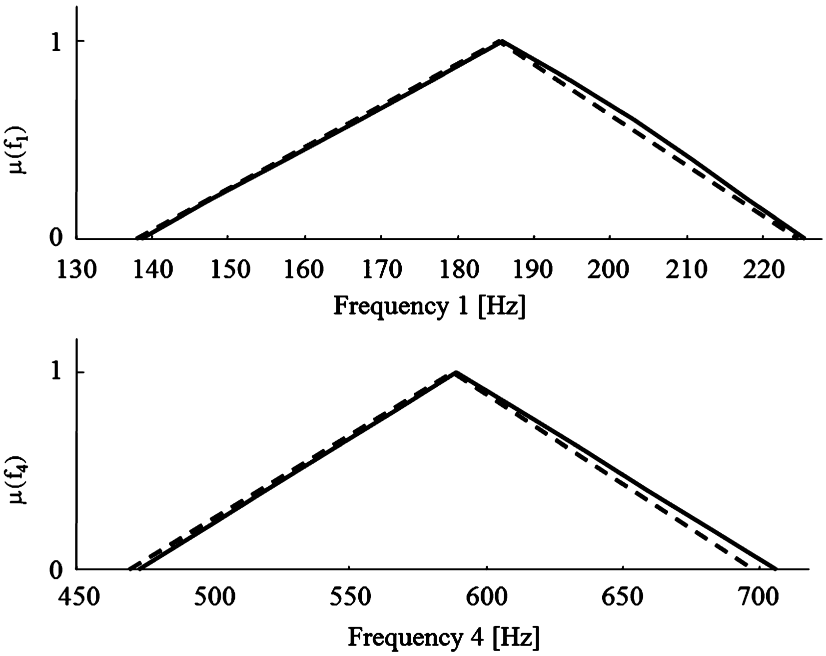

Fig. 18. A comparison of the membership functions of the numerical and experimental frequencies f_1 and f_4 (for e_1 and e_2 only). —— Numerical frequencies – – – Experimental frequencies.

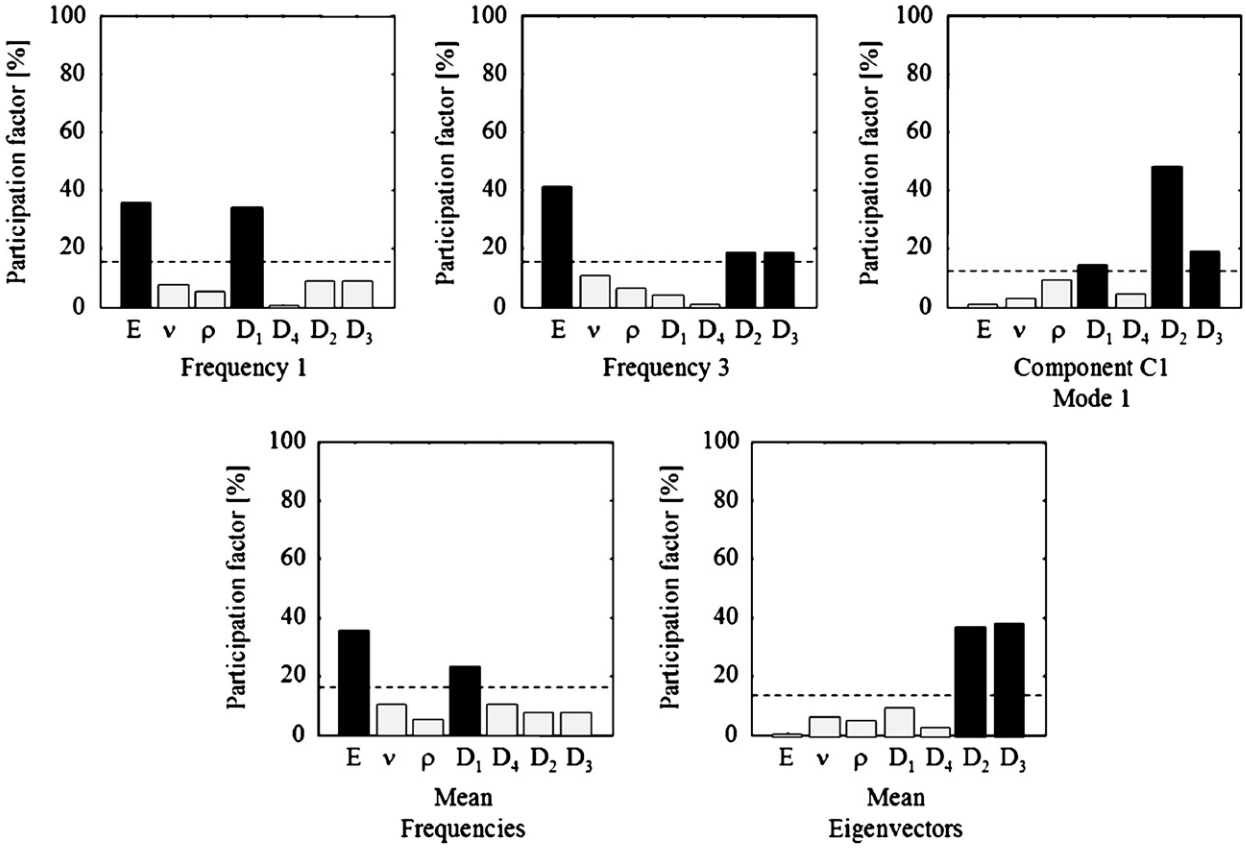

Fig. 19. Influence of the other imprecise parameters on the frequencies f_1 and f_3, on the first mode shape of component C1, and on the mean frequency and mean eigenvector (without e_1 and e_2).

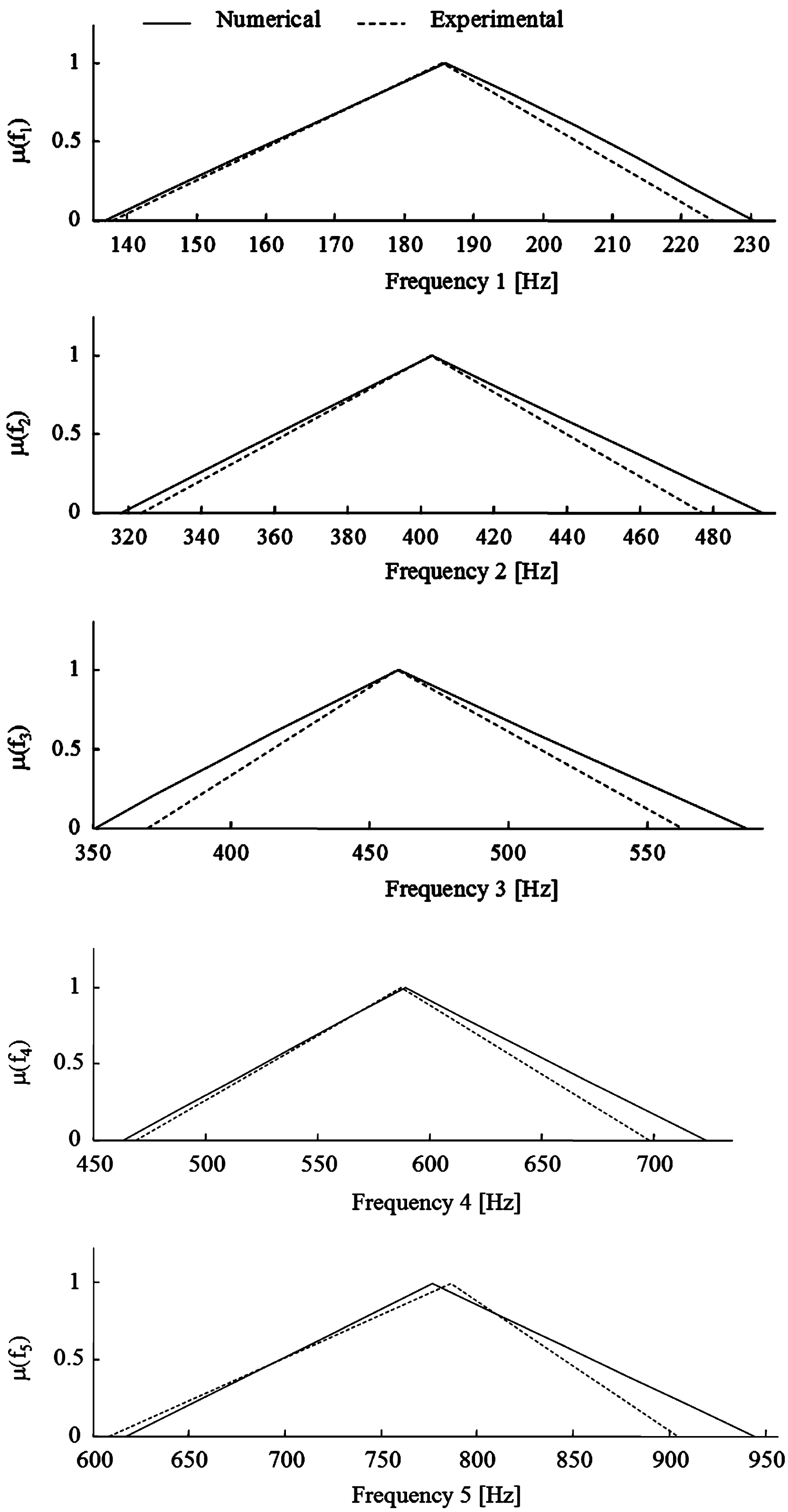

Fig. 20. Comparison of the membership functions of the numerical and experimental frequencies. —— Numerical frequencies – – – Experimental frequencies.

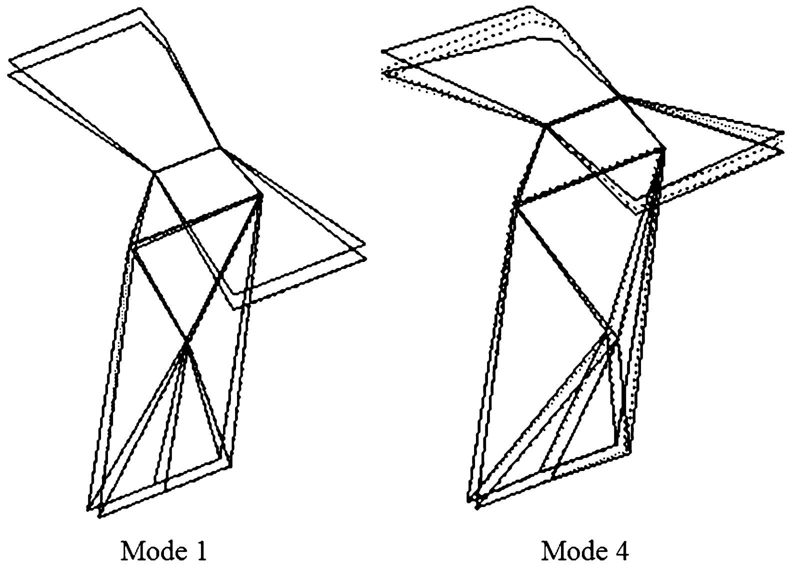

Fig. 21. Comparison of numerical and experimental mode shapes in term of lower and upper bounds. — Experimental modes shapes - - - Numerical modes shapes.

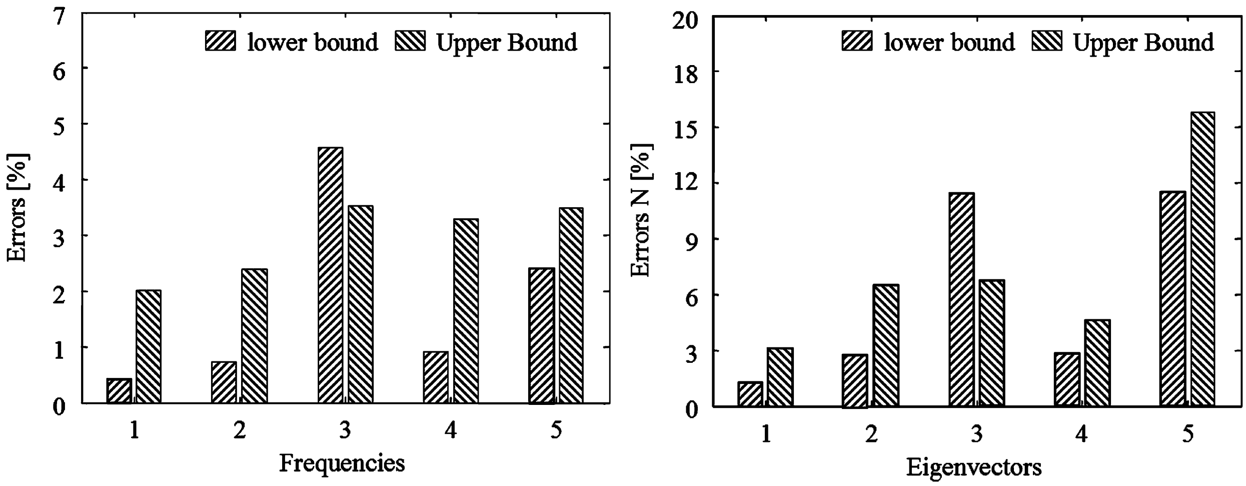

Fig. 22. Errors made in determining the lower and upper frequency and eigenvector bounds. Lower bounds. Upper bounds.

This fuzzy numerical model is an improvement on deterministic models. Using this model, the different results can be aggregated using a fuzzy formalism, providing fuzzy solutions that show both the evolution and the robustness of the studied quantities in terms of the variations in the input parameters. Future experiments will focus on evaluating fuzzy transfer functions.

Acknowledgments

The present research work has been supported by International Campus on Safety and Intermodality in Transportation the Nord-Pas-de-Calais Region, the European Community, the Regional Delegation for Research and Technology, the Ministry of Higher Education and Research, and the National Center for Scientific Research. The authors gratefully acknowledge the support of these institutions.

Appendix A. PAEM algorithm

The PAEM algorithm (Fig. 23) consists of the following steps:
For the crisp values ($\alpha = 1$):

- Determine the modal quantities and their first sensitivities for each fuzzy parameter. The signs of the first-order sensitivities indicate the functional dependence of the response function and define the combinations of discrete fuzzy parameter values for the following α-cut level, which could supply the minimum and maximum variations (Step 1).
  For each α-cut level:

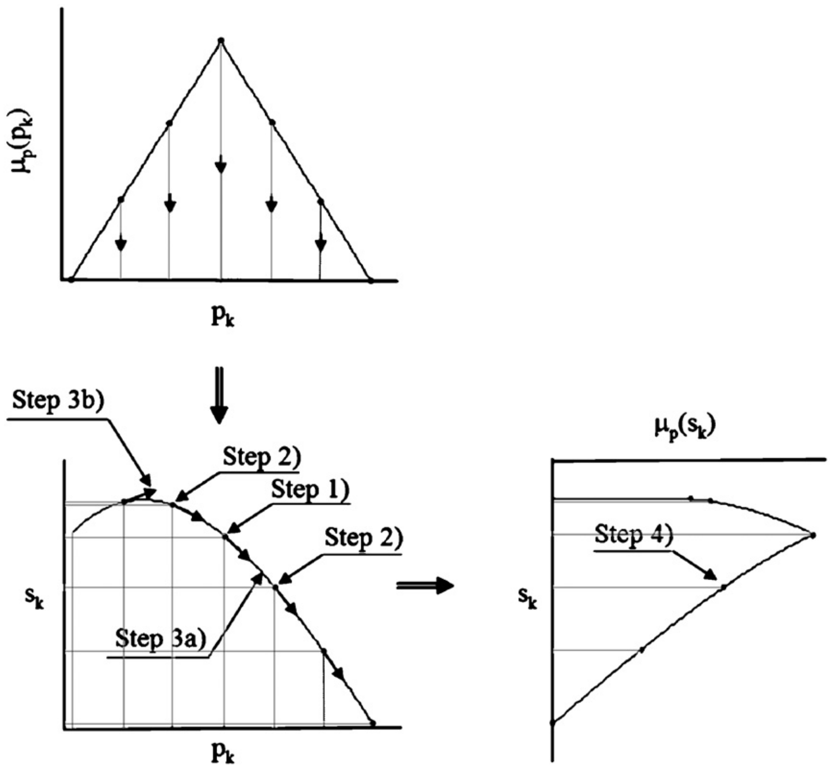

Fig. 23. Construction of fuzzy number solution $\tilde{s}_k$.

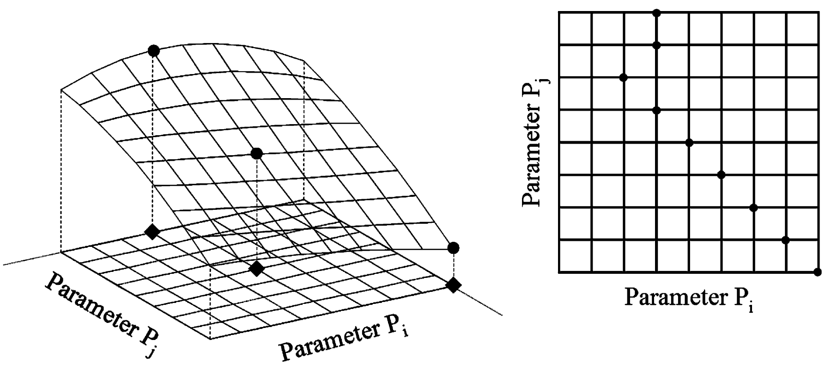

Fig. 24. Graphical representation of PAEM method in the parameter space.

- Evaluate the first derivatives of the modal quantities for the combinations of discrete fuzzy parameter values determined at the previous α-cut level (Step 2).
- Compare the signs of the derivatives with those obtained at the previous α-cut level.
  - If the sensitivities have the same signs, the response function is considered to be locally monotonic, and the determined combinations provide the minimum and maximum variations of the modal quantities for the current α-cut level (Step 3a).
  - If the sensitivities have different signs, the response function cannot be considered as monotonic, giving rise to an extremum between these two α-cut levels. The combination nearest the extremum is chosen and the search is stopped for this variation (Step 3b).
- Calculate the eigensolutions for the selected combinations of discrete fuzzy parameter values and apply the MAC criterion to verify the form of the modes. To decrease the calculation time and maintain a good level of accuracy, the "exact" calculation (corresponding to a deterministic finite element simulation) is replaced by a high-order approximation using Padé rational functions.

Finally, the graphical representation of the calculations of combinations of values of parameters of PAEM method is presented in Fig. 24 in the case of two parameters. Compared to Fig. 13, it can be seen in Fig. 24 that the non-monotonic functional dependence is taken into account.

References

[1] D. Moens, D. Vandepitte, A survey of non-probabilistic uncertainty treatment in finite element analysis, *Computer Methods in Applied Mechanics and Engineering* 194 (2005) 1527–1555.

[2] F. Massa, K. Ruffin, T. Tison, B. Lallemand, A complete method for efficient fuzzy modal analysis, *Journal of Sound and Vibration* 309 (1–2) (2008) 63–85.

[3] S.S. Rao, P. Sawyer, Fuzzy finite element approach for the analysis of imprecisely defined systems, *AIAA Journal* 33 (12) (1995) 2364–2370.

[4] M. Hanss, K. Willner, A fuzzy arithmetical approach to the solution of finite element problems with uncertain parameters, *Mechanics Research Communication* 27 (3) (2000) 257–272.

[5] M. Hanss, The transformation method for the simulation and analysis of systems with uncertain parameters, *Fuzzy Sets and Systems* 130 (2002) 277–289.

[6] F. Massa, T. Tison, B. Lallemand, A fuzzy procedure for the static design of imprecise structures, *Computer Methods in Applied Mechanics and Engineering* 195 (2006) 925–941.

[7] B. Lallemand, A. Cherki, T. Tison, P. Level, Fuzzy modal finite-element analysis of structures with imprecise material properties, *Journal of Sound and Vibration* 220 (2) (1999) 353–364.

[8] B. Lallemand, P. Plessis, T. Tison, P. Level, Neumann expansion for fuzzy finite-element analysis, *Engineering Computations* 16 (5) (1999) 572–583.

[9] F. Massa, B. Lallemand, T. Tison, P. Level, Fuzzy eigensolutions of mechanical structures, *Engineering Computations* 21 (1) (2004) 66–77.

[10] S. Donders, D. Vandepitte, J. Van de Peer, W. Desmet, Assessment of uncertainty on structural dynamic responses with the short transformation method, *Journal of Sound and Vibration* 288 (2005) 523–549.

[11] D. Moens, D. Vandepitte, On an interval finite element approach for the calculation of envelope frequency response functions, *International Journal for Numerical Methods in Engineering* 61 (14) (2004) 2480–2507.

[12] D. Moens, D. Vandepitte, A fuzzy finite element procedure for the calculation of uncertain frequency response functions of damped structures: part 1—procedure, *Journal of Sound and Vibration* 288 (3) (2005) 431–462.

[13] H. De Gersem, D. Moens, W. Desmet, D. Vandepitte, A fuzzy finite element procedure for the calculation of uncertain frequency response functions of damped structures: part 2—numerical case studies, *Journal of Sound and Vibration* 288 (3) (2005) 463–486.

[14] R.F. Nunes, A. Klimke, J.R.F. Arruda, On estimating frequency response function envelopes using the spectral element method and fuzzy sets, *Journal of Sound and Vibration* 291 (2006) 986–1003.

[15] H. De Gersem, D. Moens, W. Desmet, D. Vandepitte, Interval and fuzzy dynamic analysis of finite element models with superelements, *Computers and Structures* 85 (2007) 304–319.

[16] T. Wasfy, A. Noor, Application of fuzzy sets to transient analysis of space structures, *Finite Elements in Analysis and Design* 29 (1998) 153–171.

[17] T.Y. Chen, C.C. Shieh, Fuzzy multiobjective topology optimization, *Computers and Structures* 78 (2000) 459–466.

[18] B. Moller, W. Graf, M. Beer, Fuzzy structural analysis using α-level optimization, *Computational Mechanics* 26 (2000) 547–565.

[19] G. Plessis, B. Lallemand, T. Tison, P. Level, Fuzzy modal parameters, *Journal of Sound and Vibration* 233 (5) (2000) 797–812.

[20] T. Wasfy, A. Noor, Finite element analysis of flexible multibody systems with fuzzy parameters, *Computer Methods in Applied Mechanics and Engineering* 160 (1998) 223–243.

[21] D. Kammer, Effect of model error on sensor placement for on-orbit modal identification of large space structures, *Journal of Guidance, Control, and Dynamics* 15 (2) (1992) 334–341.
[22] H. Andriambololona, *Optimisation des essais et recalage de modèles structuraux*, Thèse de Doctorat, Université de Franche-Comté, 1990.
[23] S. Thibaud, J.C. Gelin, Influence of initial and induced hardening on the formability in sheet metal forming, *Material Processing Defects* (2002) 505–520.
[24] L.A. Zadeh, Fuzzy sets, *Information and Control* 8 (1965) 338–353.
[25] L.A. Zadeh, The concept of a linguistic variable and its application to approximate reasoning—part I, *Information Sciences* 8 (1975) 199–249.
[26] L.A. Zadeh, The concept of a linguistic variable and its application to approximate reasoning—part II, *Information Sciences* 8 (1975) 301–357.
[27] L.A. Zadeh, The concept of a linguistic variable and its application to approximate reasoning—part III, *Information Sciences* 8 (1975) 43–80.
[28] S. Valliappan, T.D. Pham, Fuzzy finite element analysis of a foundation on an elastic soil medium, *International Journal for Numerical and Analytical Methods in Geomechanics* 17 (1993) 771–789.
[29] S. Valliappan, T.D. Pham, Elasto-plastic finite element analysis with fuzzy parameters, *International Journal for Numerical and Analytical Methods in Engineering* 38 (1995) 531–548.
[30] W.M. Dong, H.C. Shah, Vertex method for computing functions of fuzzy variables, *Fuzzy Sets and Systems* 24 (1) (1987) 65–78.
[31] A. Elhage-Hussein, M. Potier-Ferry, N. Damil, A numerical continuation method based on Padé approximants, *International Journal of Solids and Structures* 37 (2000) 6981–7001.
[32] E. Foltete, Méthode dite de lissage linéaire, E. Foltete, R. Fillod, G. Lallement, J. Piranda, J.L. Raynaud, *Notice d'utilisation de programme Modan PC Version 3.0*, Université de Franche-Comté, 2002.